6982–6991 *Nucleic Acids Research, 2005, Vol. 33, No. 22*
doi:10.1093/nar/gki999

Coupling DNA-binding and ATP hydrolysis in *Escherichia coli* RecQ: role of a highly conserved aromatic-rich sequence

Morgan C. Zittel and James L. Keck*

Department of Biomolecular Chemistry, 550 Medical Science Center, 1300 University Avenue, University of Wisconsin Medical School, Madison WI 53706-1532, USA

Received August 15, 2005; Revised November 4, 2005; Accepted November 15, 2005

ABSTRACT

RecQ enzymes are broadly conserved Superfamily-2 (SF-2) DNA helicases that play critical roles in DNA metabolism. RecQ proteins use the energy of ATP hydrolysis to drive DNA unwinding; however, the mechanisms by which RecQ links ATPase activity to DNA-binding/unwinding are unknown. In many Superfamily-1 (SF-1) DNA helicases, helicase sequence motif III links these activities by binding both single-stranded (ss) DNA and ATP. However, the ssDNA-binding aromatic-rich element in motif III present in these enzymes is missing from SF-2 helicases, raising the question of how these enzymes link ATP hydrolysis to DNA-binding/unwinding. We show that *Escherichia coli* RecQ contains a conserved aromatic-rich loop in its helicase domain between motifs II and III. Although placement of the RecQ aromatic-rich loop is topologically distinct relative to the SF-1 enzymes, both loops map to similar tertiary structural positions. We examined the functions of the *E.coli* RecQ aromatic-rich loop using RecQ variants with single amino acid substitutions within the segment. Our results indicate that the aromatic-rich loop in RecQ is critical for coupling ATPase and DNA-binding/unwinding activities. Our studies also suggest that RecQ's aromatic-rich loop might couple ATP hydrolysis to DNA-binding in a mechanistically distinct manner from SF-1 helicases.

INTRODUCTION

DNA helicases play central roles in essentially every pathway of DNA metabolism. These ubiquitous molecular motors couple nucleoside 5′ triphosphate (NTP) binding and hydrolysis to double stranded (ds) nucleic acid unwinding, which produces single-stranded (ss) DNA required for processes such as replication, recombination and repair. Helicases have been grouped into superfamilies based primarily upon conservation of helicase sequence motifs I, Ia, II, III, IV, V and VI (1) (Figure 1A). Helicase Superfamilies 1 and 2 (SF-1 and SF-2) possess all seven of these characteristic motifs; in crystal structures of SF-1 and -2 helicases these motifs line the walls of a cleft formed by the intersection of two RecA-like domains (1–3). Motifs I and II share significant conservation between SF-1 and SF-2 helicases, whereas the remaining motifs are less highly conserved and demarcate the SF-1 and SF-2 helicases (1,2). Together, the helicase motifs mediate DNA-binding, NTP-binding and hydrolysis, and DNA unwinding, although for most helicases the exact manner in which the helicase motifs function in these processes are poorly understood (3).

Coordination of DNA-binding and ATP hydrolysis is a feature that appears to be uniformly conserved among DNA helicases. As a result of extensive structural and biochemical analyses, DNA-binding and ATP hydrolysis 'coupling' roles for a number of the conserved helicase motifs have been inferred (3). In particular, studies of the highly-homologous PcrA-related SF-1 helicases (PcrA, Rep and UvrD) have demonstrated a clear importance for motif III in linking DNA-binding to ATP hydrolysis (4–11). In crystal structures of PcrA and Rep helicases bound to DNA, the C-terminal half of motif III forms an aromatic-rich loop that directly binds single-stranded (ss) DNA via stacking of aromatic residues with bases of the ssDNA and through electrostatic contacts between an arginine residue and the ssDNA phosphodiester backbone (9,12) (Figure 1B–D). In substrate- and product-bound crystal forms of PcrA, the aromatic-rich loop is directly C-terminal to a motif III glutamine residue that contacts the ATP γ-phosphate and a sulfate ion (thought to mimic an inorganic phosphate), respectively (7,12). These observations have led to a model in which the glutamine in motif III acts as a sensor of ATP versus ADP-binding, thereby

*To whom correspondence should be addressed. Tel: +608 263 1815; Fax: +608 262 5253; Email: jlkeck@wisc.edu

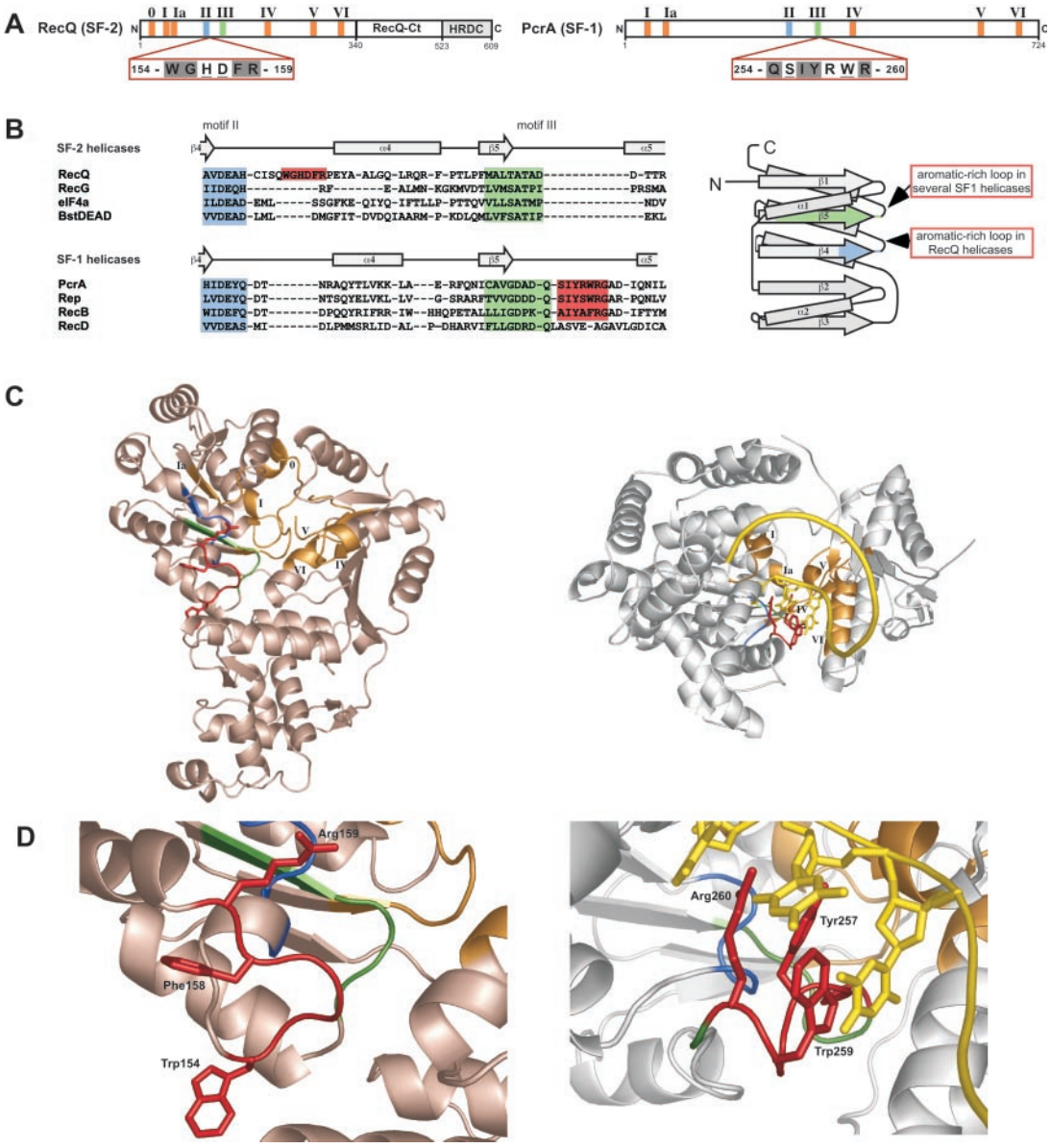

Figure 1. Aromatic-rich loops in helicase structures. (**A**) Schematic diagram highlighting conservation and location of aromatic-rich loops in RecQ and PcrA proteins. Shaded or underlined residues are invariant or highly conserved, respectively, in all RecQ or PcrA protein sequences examined. Helicase motifs II and III are colored blue and green, respectively, and all other helicase motifs are colored orange. Two non-helicase domains are identified in the RecQ diagram (RecQ-Ct and HRDC). (**B**) (Left) Structure-based sequence comparison of representative SF-2 (top) and SF-1 (bottom) helicases. The structures of several helicases, or helicase domains, were superimposed using FSSP (30) and the structurally aligned sequences from motif II through motif III are shown. Schematic diagrams of the secondary structure of the RecQ (top) and the PcrA (bottom) structures are shown with color coding as in (A) for motifs II and III and aromatic-rich loops boxed in red. The helicase structures shown are: RecQ [(pdb code 1OYW, (14)], RecG [1GM5, (27)], eIF4a [1FUU, (31)], BstDEAD helicase domain [1Q0U, (32)], PcrA [3PJR, (12)], Rep [1UAA, (9)], RecB and RecD [1W36D, (13)] (Right) Generalized topology diagram of the N-terminal helicase domain [adapted from (3)] colored as in (A) to indicate the positions of motifs II and III and with arrows pointing to the positions of the aromatic-rich loops in RecQ or in several SF-1 helicases. (**C**) Comparison of aromatic-rich loops in RecQ (left) and PcrA (right). The crystal structures were overlaid by aligning β-strands in the N-terminal helicase domains from RecQ and PcrA and translated for visualization. Conserved helicase motifs are indicated and colored as in (A). Aromatic-rich loops are shown in red and DNA is shown in yellow. (**D**) Close-up of aromatic-rich loops shown in (C).

altering DNA-binding affinity through subtle conformational changes within the aromatic-rich loop (6). Consistent with this model, mutations made within PcrA's aromatic-rich loop lead to impairment of ATP hydrolysis, DNA-binding, duplex DNA unwinding or a combination of these deficiencies (5,6). Thus, it has been suggested that the PcrA aromatic-rich loop serves to couple the energy released by ATP hydrolysis to DNA unwinding through direct contacts with both the DNA substrate and ATP (6). Similarly, mutagenesis of UvrD motif III residues located upstream of its aromatic-rich loop further indicate a role for motif III in coupling ATPase function and DNA-binding (10,11). In these studies, two residues in motif III [the equivalent phosphate-binding glutamine to that in PcrA and a nearby aspartate (Figure 1B)] were individually mutated and found to decouple ATP- and DNA-binding. Similar aromatic-rich loops are found in other SF-1 helicases

[e.g. RecB (13), Figure 1B], although exceptions lacking this element also exist [e.g. RecD (13)]. Thus, substantial evidence indicates that motif III in PcrA-related enzymes (and most likely in many other SF-1 helicases) serves as a coupling element, linking DNA-binding and ATPase activities.

SF-1 helicases serve as valuable models for understanding the mechanisms of both SF-1 and SF-2 helicases. Comparison of the crystal structure of the catalytic core domain of *Escherichia coli* RecQ, a SF-2 helicase, to available crystal structures of PcrA and Rep has revealed many parallels among the helicases despite their membership in different superfamilies (9,12,14). However, one striking difference between RecQ and the PcrA-related structures is that motif III of RecQ does not contain an aromatic-rich loop (Figure 1). Instead, RecQ presents a surface exposed aromatic-rich loop between motifs II and III (Trp154-Arg159). While the function of this aromatic-rich loop in RecQ is not clear, its high degree of conservation among RecQ family members suggests that it plays an important role in RecQ function.

In this report, we test the hypothesis that the aromatic-rich loop in *E.coli* RecQ fills a similar role to that played by the analogous loop in PcrA-related helicases. Residues Trp154, Phe158 and Arg159 from the RecQ aromatic-rich loop were mutated and the variant proteins were tested for their abilities to hydrolyze ATP and bind and unwind duplex DNA. Our results indicate that the aromatic-rich loop in *E.coli* RecQ is important for coupling the enzyme's ATPase and DNA-binding/unwinding functions. Moreover, Trp154, Phe158 and Arg159 are all shown to contribute to RecQ's ability to translate the energy released by ATP hydrolysis into productive DNA unwinding. These data support a model in which the RecQ aromatic-rich loop couples ATP hydrolysis to DNA-binding/unwinding, akin to the aromatic-rich loops of the PcrA-related enzymes.

MATERIALS AND METHODS

Subcloning, over-expression and purification of *E.coli* RecQ Proteins

A T7-over-expression plasmid encoding the *E.coli* RecQ sequence preceded by a His_6 affinity-purification element was described previously (15). Mutant RecQ over-expression vectors were constructed using the QuikChange site-directed mutagenesis kit (Stratagene) according to the manufacturer's instructions. Mutant W154L was generated with primers W154L_Fwd_2 (5′-GCA CTG TAT CTC CCA ATT GGG CCA CGA TTT CCG-3′) and W154L_Rev_2 (5′-CGG AAA TCG TGG CCC AAT TGG GAG ATA CAG TGC-3′). Mutant F158L was generated with primers F158L_for (5′-CAA TGG GGC CAC GAT CTG CGC CCG GAA TAT GCC-3′) and F158L_rev (5′-GGC ATA TTC CGG GCG CAG ATC GTG GCC CCA TTG-3′). Mutant R159L was generated with primers R159L_Fwd (5′-TGG GGC CAC GAT TTC CTG CCG GAA TAT GCC GCG-3′) and R159L_Rev (5′-CGC GGC ATA TTC CGG CAG GAA ATC GTG GCC CCA-3′). Mutant Y162L was generated with primers Y1562L_for (5′-GAT TTC CGC CCG GAA CTG GCC GCG CTC GGT CAG-3′) and Y162L_rev (5′-CTG ACC GAG CGC GGC CAG TTC CGG GCG GAA ATC-3′). The fidelity of wild-type (WT) and mutant *recQ* genes was confirmed by DNA sequencing.

Cultures of BL21(DE3) *E.coli* cells transformed with pLysS (Novagen) and pET15_RecQ, pW154L, pF158L, pR159L or pY162L were grown at 37°C in Luria–Bertani medium (16) supplemented with 100 μg/ml ampicillin and 25 μg/ml chloramphenicol. Cells at an $OD_{600\ nm}$ of 0.5–0.6 were induced to over-express RecQ (or a RecQ variant) by the addition of 1 mM isopropyl β-D-thiogalactopyranoside and were harvested by centrifugation after an additional 2.5 h of growth. Cells were suspended in lysis buffer [20 mM Tris (pH 8.0), 20 mM imidazole (pH 8.0), 300 mM NaCl, 1 mM β-mercaptoethanol, 10% v/v glycerol and 100 mM dextrose] and lysed by sonication on ice. All subsequent purification steps were performed at 4°C. Soluble lysate was loaded on a Ni^{2+}–NTA column and washed with lysis buffer; His-tagged protein was eluted by the addition of 20 mM Tris (pH 8.0), 100 mM imidazole (pH 8.0), 300 mM NaCl, 1 mM β-mercaptoethanol and 10% v/v glycerol. Eluent was dialyzed against lysis buffer without imidazole, digested with thrombin to remove the His-tag (a Gly-Ser-His sequence remains on the N-terminus) and passed over a Ni^{2+}–NTA column a second time to remove the His-tag and any contaminating proteins. The protein solution was diluted to 100 mM NaCl using buffer containing 20 mM Tris (pH 8.0), 1 mM β-mercaptoethanol, 1 mM EDTA and 10% v/v glycerol, loaded on to a MonoQ column (Pharmacia), and eluted with a linear NaCl gradient from 120 to 300 mM. Purified fractions of each protein were pooled, concentrated to >1 mg/ml, dialyzed against 20 mM Tris (pH 8.0), 300 mM NaCl, 1 mM β-mercaptoethanol, 1 mM EDTA and 40% v/v glycerol, and stored at −20°C. Protein concentrations were determined by measuring their $A_{280\,nm}$ in 6.0 M guanidine–HCl (17) (1 $OD_{280\,nm} = 21.2$ μM for RecQ, F158L and R159L, 24.1 μM for W154L, and 21.8 μM for Y162L). Proper folding of variant proteins was evaluated by limited proteolysis as described previously (15).

Limited proteolysis

E.coli RecQ (3.5 μM) was incubated with 0.035 μM protease (α-chymotrypsin, trypsin or subtilisin) in 20 mM Tris (pH 8.0), 150 mM NaCl, 1 mM β-mercaptoethanol, 1 mM EDTA at room temperature. In reactions involving nucleotide, 0.1 mM ADP or AMPPNP was added to the reaction. In reactions involving DNA, 1.5 μM DNA was added to the reaction. ssDNA was a 30 base ssDNA (oligo 1: 5′-GCG TGG GTA ATT GTG CTT CAA TGG ACT GAC-3′) and the 3′ overhang (3′OH) DNA substrate was created by annealing oligo 1 to an 18 nt long oligonucleotide (oligo 2: 5′-AAG CAC AAT TAC CCA CGC-3′), which resulted in an 18 bp region and a 12-base 3′ ss extension. Aliquots (10 μl) from the reaction were quenched by mixing with 10 μl 2× loading dye [63 mM Tris (pH 6.8), 2% SDS, 10% glycerol, 710 mM β-mercaptoethanol and 0.005% bromophenol blue] and freezing on dry ice. Samples were boiled followed by separation by SDS–PAGE on 10 or 15% gels and stained with Coomassie brilliant blue.

ATPase assays

Two variations of ATPase assays were performed. To compare DNA-dependent ATP hydrolysis profiles, purified RecQ

variants were mixed with 0–1000 nM dT_{28} in 20 mM HEPES (pH 8.0), 50 mM NaCl, 1 mM β-mercaptoethanol, 2 mM $MgCl_2$, 0.1 g/l BSA, 1 mM ATP, at 25°C. WT RecQ protein concentrations were 1, 5 or 50 nM and concentrations of the W154L, F158L and R159L variants were 5 or 50 nM. To compare the effects of ATP concentration on ATP hydrolysis roles, 50 nM of each variant protein was mixed with 0–4.55 mM ATP in 20 mM HEPES (pH 8.0), 50 mM NaCl, 1 mM β-mercaptoethanol, 1 mM $MgCl_2$, 0.1 g/l BSA and 100 nM dT_{28}, at 25°C. Both ATPase assay variations also included an ATP regeneration system that converts ADP–ATP in a reaction that is coupled to the conversion of NADH to NAD^+ (18). This coupled reaction can be detected spectrophotometrically by observing the decrease of $A_{340\ nm}$ due to NADH oxidation. Steady-state $\Delta A_{340\ nm}/\Delta t$ rates were measured and converted to $\Delta[ATP]/\Delta t$ to determine the ATPase rates and were normalized to the concentration of RecQ present in each reaction. K_m and k_{cat} values were derived by fitting ATPase activity resulting from ATP titrations to the Michaelis–Menten equation (KaleidaGraph 3.6), rate $= (V_{max} \times [ATP])/(K_m + [ATP])$. k_{cat} values were calculated by dividing V_{max} values by the concentration of the RecQ variant in the reaction. K_{DNA} values are the concentration of DNA at which each enzyme was half-maximally stimulated. Measurements are reported in triplicate and error bars represent 1 SD of the mean.

DNA-binding assay

A 3′-fluorescein-conjugated 30 base ssDNA (oligo 1) was the DNA substrate for assays measuring binding to ssDNA. For assays measuring binding to a 3′OH, 3′-fluorescein-conjugated oligo 1 was annealed to non-labeled oligo 2. RecQ proteins were diluted serially from 1000 to 0.01 nM into 20 mM Tris (pH 8.0), 50 mM NaCl, 4% v/v glycerol, 1 mM $MgCl_2$, 1 mM β-mercaptoethanol and 0.1 g/l BSA. Dilutions of RecQ proteins were incubated for 5 min at room temperature with 200 pM substrate in a total volume of 100 µl. The fluorescence polarization of each sample was measured at 25°C with a Beacon 2000 fluorescence polarization system. Measurements are reported in triplicate and error bars represent one SD of the mean. Uncertainties reported with apparent K_d values are one SD of the mean.

Helicase assays

The DNA substrate was created by phosphorylating the 5′ end of oligo 2 in a T4 polynucleotide kinase reaction with [γ-^{32}P]ATP and annealing phosphorylated oligo 2 and oligo 1 by boiling and slowly cooling an equimolar mixture, resulting in a radiolabeled 3′OH molecule. The substrate was purified via native PAGE on a 12% gel followed by electroelution and dialysis against 20 mM Tris (pH 8.0) and 50 mM NaCl. Purified RecQ variants were incubated with substrate (~1 nM mol) in 20 mM Tris (pH 8.0), 50 mM NaCl, 1 mM β-mercaptoethanol, 1 mM $MgCl_2$, 1 mM ATP, 0.1 g/l BSA, 4% v/v glycerol for 30 min at 25°C with protein concentrations between 0.0001 and 100 nM. Reactions were terminated by addition of 11% v/v glycerol, 0.28% SDS (to denature RecQ) and 5 ng unlabeled oligo 2 (to prevent reannealing of the unwound radiolabeled DNA). The helicase products were analyzed by PAGE on a 12% non-denaturing gel, dried onto Whatman paper, and visualized using a phosphorimager.

RESULTS

Helicase sequence comparisons for aromatic-rich loops

In an effort to identify mechanistically important elements of the *E.coli* RecQ protein, we compared its catalytic core structure (14) to other well-studied helicases with defined three-dimensional structures (Figure 1B–D). The major difference was the presence of an aromatic-rich polypeptide loop encoded between motifs II and III in RecQ that is absent from other helicase structures (Figure 1). This loop is positioned at the interface between the two lobes of the enzyme's helicase domain and is highly conserved among bacterial and eukaryotic RecQ family members (14). Interestingly, this loop is not present in other SF-2 helicases (Figure 1B). These features led us to postulate that the loop could be an important contributor to RecQ helicase mechanisms.

Additional searches for aromatic-rich loop segments encoded by different regions in non-RecQ helicase domains identified a loop conserved in several SF-1 helicases (PcrA, Rep, UvrD and RecB) that forms the C-terminal portion of helicase motif III (4,9,12) (Figure 1B). This loop is absent from motif III of SF-2 helicases and is not found in the structures of all SF-1 enzymes (e.g. RecD, Figure 1B). Motif III sequences of several other SF-1 enzymes (including *E.coli* TraI and *Saccharomyces cerevisiae* Dna2 and Pif1) lack an apparent aromatic-rich loop as well (data not shown). However, as with the RecQ loop, the SF-1 aromatic-rich loop is well conserved within given helicase subfamilies and maps to the cleft of the helicase domain. Furthermore, in spite of the fact that RecQ and the PcrA-related and RecB enzymes encode aromatic-rich loops in different parts of their respective primary structures, these loops map to very similar tertiary structural positions. Motif III residues found both within and outside of the aromatic-rich loop of PcrA-related enzymes have been shown to be important for coordinated ATP hydrolysis and DNA-binding/unwinding (4–11). The proven mechanistic importance of the PcrA-related enzyme loop led to an investigation of the role of the aromatic-rich loop in RecQ helicases.

Purification and limited proteolysis of *E.coli* RecQ aromatic-rich loop variants

To test the possible functional importance of residues within the aromatic-rich loop, four recombinant *E.coli* RecQ variant proteins with single-residue substitutions were over-expressed and purified. Three aromatic residues, Trp154, Phe158 and Tyr162, and one basic residue, Arg159, were converted to leucines due to predicted structural contributions of the C_α-proximal portions of each side chain to the hydrophobic core of the protein. Arg159 was included in this panel of mutants because of a similarly placed Arg in the PcrA aromatic-rich loop (Figure 1A).

To examine whether the RecQ variants were properly folded, limited proteolysis experiments were performed on each of the purified proteins. Because the point mutations were within the catalytic core domain, it was predicted that any destabilizing effects of the mutations would lead to

changes in the variant's proteolysis pattern relative to the pattern described for WT RecQ (15). In all cases but one, the proteolysis patterns were indistinguishable from that of WT RecQ (data not shown). However, the Y162L RecQ variant was rapidly proteolyzed and did not form the proteolytically resistant catalytic core domain characteristic of properly folded *E.coli* RecQ protein (15). Thus, three of the variants appeared to be properly folded whereas the fourth, Y162L, is likely to have been improperly folded and was omitted from further biochemical analysis.

DNA-dependent ATPase activities of WT and variant RecQ proteins

To test the hypothesis that residues in the RecQ aromatic-rich loop are involved in ATP hydrolysis and DNA-binding, we measured the DNA-dependent ATP hydrolysis activity of the aromatic-rich loop mutants using a spectrophotometric ATPase assay (18) and compared them to WT RecQ. WT RecQ has a weak ATPase activity that is greatly stimulated by DNA (15,19). The ability of RecQ to unwind dsDNA precludes the use of dsDNA as a cofactor in this assay since ssDNA and dsDNA differ in their ability to stimulate ATP hydrolysis by RecQ (15,19). To circumvent this limitation, a ssDNA homopolymer cofactor (dT_{28}) was titrated into the reactions to allow measurement of ATP hydrolysis on a homogeneous DNA structure. Consistent with previous results (15,19), WT RecQ has limited ATPase activity in the absence of DNA but can be stimulated over 200-fold upon addition of DNA, reaching a rate of 1340 ± 120 min^{-1} (Figure 2A and B).

If residues within the RecQ aromatic-rich loop are involved in coupling ATP hydrolysis to DNA-binding/unwinding, we predict that mutation of these residues would lead to deficiencies in ATPase and DNA-binding/unwinding activities. Consistent with this prediction, mutation of either residue R159 or W154 produced RecQ variants that require significantly higher concentrations of dT_{28} to stimulate their ATPase activities (K_{DNA}) relative to WT (Figure 2A and Table 1). Both the R159L and W154L variants also displayed reduced maximal ATPase rates at nearly saturating dT_{28} concentrations relative to WT (Figure 2A).

The F158L variant ATPase activity was radically altered relative to WT RecQ and the other variants tested. Surprisingly, the F158L variant displayed robust ATPase activity in the absence of a DNA cofactor, with a rate of 90 min^{-1} (Figure 2A and B). To our knowledge this is the first observation of significant DNA-independent ATPase activity by a RecQ helicase. Addition of dT_{28} only mildly stimulated F158L ATPase activity over its DNA-independent levels (~7-fold stimulation), which allowed this variant to reach a maximal rate approximately one-half that of WT. Interestingly, although the stimulatory effect of ssDNA on F158L ATPase activity was modest in comparison to that of WT, both required the same dT_{28} concentrations for half-maximal stimulation (Table 1). In contrast, the R159L and W154L variants required ~3- to 4-fold higher ssDNA concentrations for half-maximal stimulation (Table 1). Thus, two effects on ATPase activity were observed for the RecQ variants: (i) decreased ATPase activity with higher ssDNA concentration requirements and (ii) a gain of function in the F158L variant that led to DNA-independent ATP hydrolysis.

ATPase kinetics of WT and variant *E.coli* RecQ proteins

We next examined the variants' steady-state ATP hydrolysis kinetics to further test the role of each residue in RecQ's mechanism of ATP hydrolysis. ATP was titrated into reactions containing 100 nM dT_{28} and 50 nM RecQ variant protein. The resulting ATPase rates were fit to the Michaelis–Menten equation as described in Materials and Methods. The k_{cat} and K_m values derived for WT RecQ ATPase kinetics were 1600 ± 200 min^{-1} and 120 ± 20 μM, respectively (Table 1). All three of the RecQ variants tested displayed modestly reduced K_m and k_{cat} kinetic parameters relative to WT protein (Table 1).

Equilibrium DNA-binding of WT and variant RecQ proteins

Each of the variant RecQ proteins tested proved to be defective in ssDNA-dependent ATP hydrolysis (Figure 2), which could have resulted from an impairment of ssDNA-binding. To test this possibility, equilibrium DNA-binding studies were used to measure binding of WT and variant proteins to fluorescently labeled ssDNA substrates. Interestingly, mutation of Trp154, Phe158 or Arg159 had no measurable effect on the apparent ssDNA-binding affinity of the RecQ variants (Figure 3). A partial-duplex DNA with a 3′ ssDNA tail (3′OH) substrate was substituted for ssDNA in a similar experiment because this is the preferred substrate for WT RecQ unwinding (20). Again, the variants' abilities to bind the 3′OH substrate were not significantly altered (data not shown). Thus, mutations in RecQ's aromatic-rich loop do not appear to significantly perturb its equilibrium DNA-binding properties.

Helicase activities of WT and variant RecQ

Helicase activities among the RecQ variants were compared by assessing unwinding of a radiolabeled 3′OH substrate in the presence of 1 mM ATP/$MgCl_2$. Because helicase activity requires proper coupling of ATP hydrolysis with DNA strand separation, unwinding assays provide a useful test of the variants' abilities to integrate these processes. Consistent with previous results (15), WT RecQ was able to unwind a 3′OH substrate in a concentration-dependent manner and displayed half-maximal unwinding at ~0.01 nM enzyme (Figure 4). However, individual mutation of residues Trp154, Phe158 and Arg159 resulted in dramatically reduced unwinding activities. Of these three mutants, only the F158L variant was competent to unwind 3′OH DNA, although it required ~1 nM enzyme to unwind 50% of the substrate, ~100-fold more than WT RecQ. Despite its ability to hydrolyze ATP in the absence of DNA (Figure 2A), the F158L variant was not able to unwind a 3′OH substrate in the absence of ATP/Mg^{2+} (data not shown). Neither the W154L nor the R159L variant was able to unwind the 3′OH substrate at even the highest enzyme concentration tested (100 nM) (Figure 4).

Limited proteolysis of WT and variant RecQ proteins with cofactors

Limited proteolysis experiments with PcrA-related helicases have shown that ssDNA and nucleotide binding protect their aromatic-rich loops from cleavage by chymotrypsin (10,11,21). Moreover, a single-site mutation in motif III in UvrD (N-terminal of the aromatic-rich loop portion of the

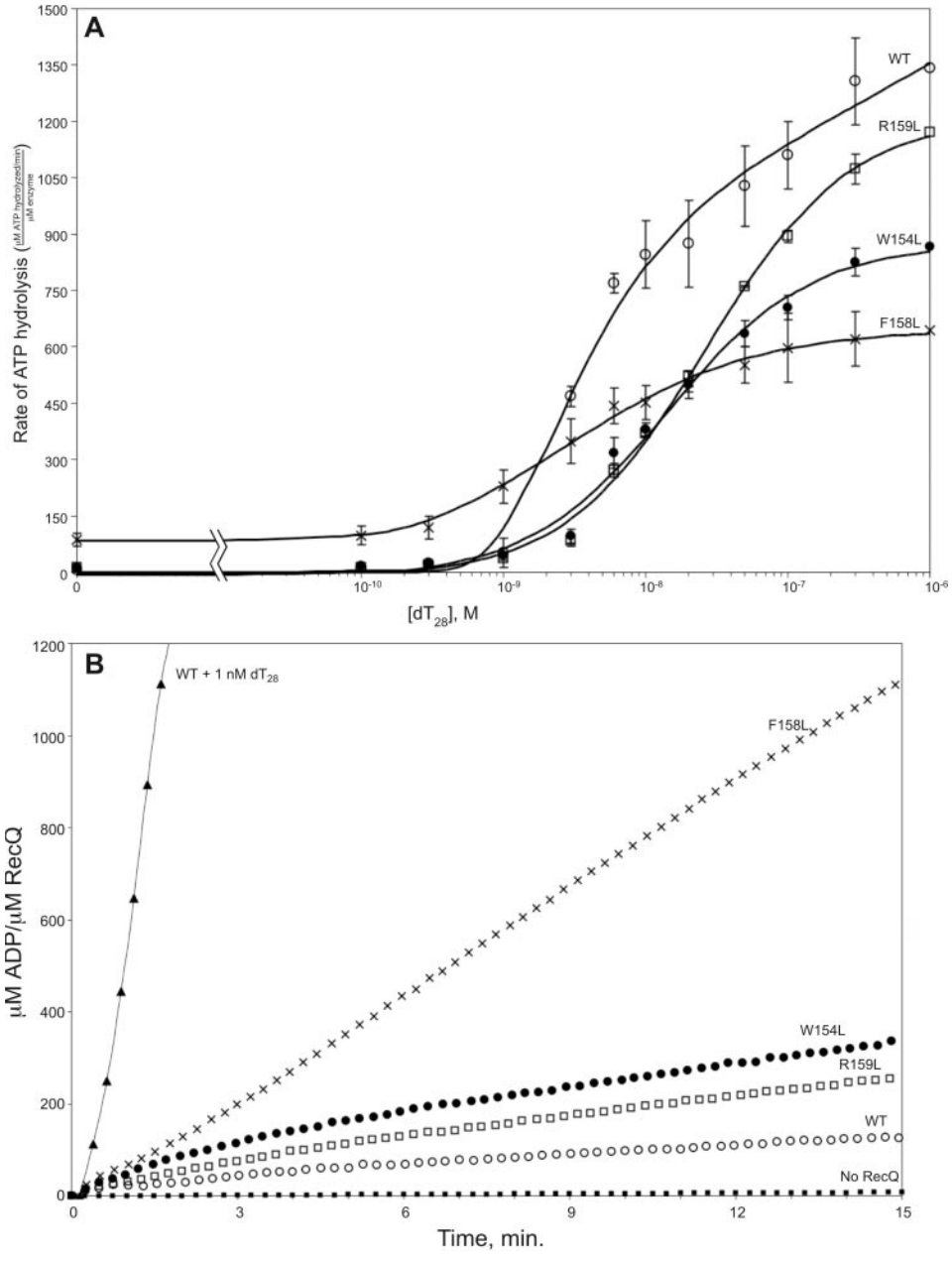

Figure 2. ATPase activity of WT RecQ (open circles), W154L (closed circles), F158L (X), and R159L (open squares). (**A**) DNA-dependent ATPase activity. WT RecQ protein concentrations were 1–50 nM, while the less active W154L, F158L and R159L variants required 5–50 nM enzyme concentrations to produce measurable ATPase rates. Data points are normalized to the specific enzyme concentration used in each measurement. Measurements are reported in triplicate and error bars represent 1 SD of the mean. (**B**) DNA-independent ATPase activity. Comparison of ATP hydrolysis by WT RecQ, W154L, F158L or R159L in the absence of DNA to that of WT RecQ with 1 nM dT_{28} (black triangles).

Table 1. Kinetic data for RecQ variant ATPase activity

	K_m (μM)	k_{cat} (min^{-1})	K_{DNA} (nM)
WT	120 ± 20	1600 ± 200	6 ± 1
W154L	80 ± 18	1000 ± 80	15 ± 1
F158L	80 ± 8	800 ± 200	4 ± 2
R159L	80 ± 19	900 ± 60	25 ± 2

K_m refers to the concentration of ATP at half-maximal activity in an ATP titration; K_m and k_{cat} were derived by fitting ATP titration data to the Michaelis–Menten equation. K_{DNA} refers to the concentration of DNA at half-maximal activity and are derived from data presented in Figure 2. All values represent an average of three trials and reported error is 1 SD of the mean.

motif) minimizes protection by nucleotide or ssDNA alone (10), indicating that ssDNA and nucleotide binding cause structural rearrangements that change the accessibility of protease-sensitive sites on the surface of these proteins. Therefore, proteases can be valuable tools for analyzing structural differences caused by mutations in helicase domains.

We used limited proteolysis to test for structural alterations induced by binding of RecQ to nucleotide or DNA cofactors. WT or variant RecQ proteins were incubated with ADP, AMPPNP (an ATP analog), a 30 nt ssDNA oligo, or a 3′OH substrate, then subjected to proteolysis by subtilisin,

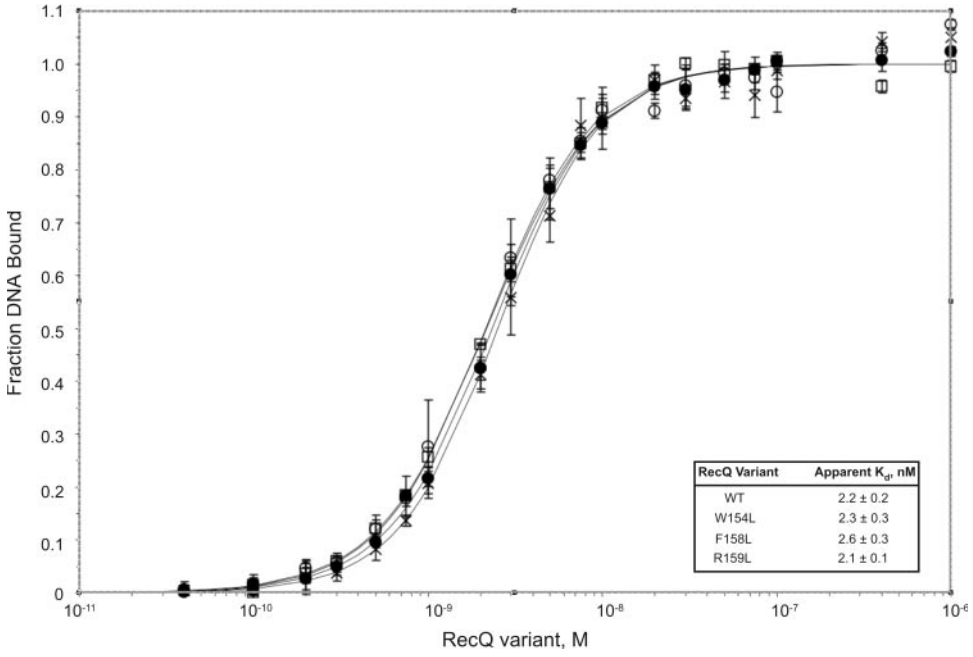

Figure 3. Equilibrium DNA-binding isotherms of WT RecQ (open circles), W154L (closed circles), F158L (X), and R159L (open squares). Inset: apparent dissociation constants for ssDNA-binding are reported as the concentration of enzyme at which 50% of DNA is bound. Measurements and K_D values are reported in triplicate and error bars represent 1 SD of the mean.

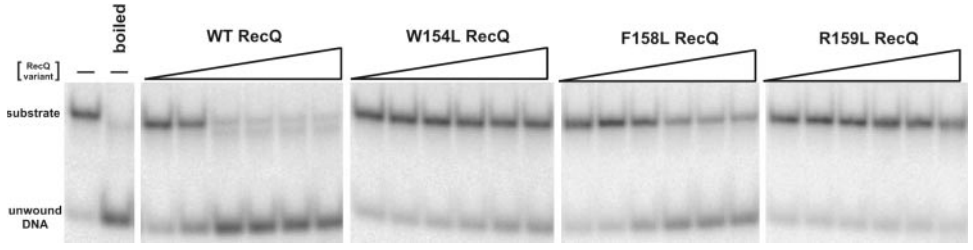

Figure 4. DNA helicase activity of WT, W154L, F158L and R159L RecQ variants. Proteins at 0.001, 0.01, 0.1, 1, 10 or 100 nM were incubated with ~1 nM radiolabeled DNA substrate as described in Materials and Methods. Unwound DNA was separated from substrate by 12% native PAGE and results were visualized using a phosphorimager. No-RecQ and boiled substrate controls are indicated. Data shown are representative of replicate experiments.

trypsin or chymotrypsin. Proteolysis of free *E.coli* RecQ results primarily in two successive cleavage events: WT RecQ (~69 kDa) is first degraded to a ~60 kDa catalytic core fragment by removal of the HRDC domain, with further proteolysis resulting in removal of ~3 kDa from the N-terminus of the catalytic core domain (15). The pattern of degradation of the free RecQ variants was identical to that of WT, although digestion of the W154L and R159L variant proteins was moderately slowed relative to the F158L variant or WT proteins (Supplementary Figure 1 and data not shown).

Previously, ADP or AMPPNP added to WT RecQ limited proteolysis reactions indicated that nucleotide addition caused an alteration in RecQ proteolysis by slowing the second proteolytic cleavage of the catalytic core (15). To test whether residues within the RecQ aromatic-rich loop altered these proteolytic patterns, ADP or AMPPNP was added to W154L, F158L or R159L variant protein before proteolytic digestion. Each variant displayed slower digestion in the presence of nucleotide cofactor than in its absence and the resulting proteolytic patterns were indistinguishable from those observed for WT RecQ (Supplementary Figure 1 and data not shown).

We further tested whether the addition or ssDNA or 3′OH DNA might alter WT or variant RecQ proteolysis patterns (Supplementary Figure 1 and data not shown). Again, digestion of WT and each variant protein from full-length protein to the catalytic core fragment was somewhat slowed in the presence of each DNA cofactor, but no change in the overall proteolytic pattern was observed. Therefore, the addition of nucleotide cofactors or DNA did not appear to alter the gross structure of *E.coli* RecQ or of the aromatic-rich loop variants.

DISCUSSION

In this report, we tested the hypothesis that an aromatic-rich loop found in the *E.coli* RecQ DNA helicase couples ATP hydrolysis to DNA-binding and unwinding. This aromatic-rich loop is similar to that of well-characterized loops in several SF-1 helicases in terms of its sequence composition and

relative tertiary structural position (Figure 1). A major difference between the aromatic-rich loops in the two helicase families is that the sequences are found in different positions in the enzymes' primary structures. In RecQ, the aromatic-rich loop is encoded between helicase motifs II and III, whereas the aromatic-rich loop in SF-1 helicases forms the C-terminal end of motif III. Structural and biochemical studies of PcrA and Rep show that this aromatic-rich loop is an important ssDNA-binding element and forms a critical physical linkage that couples DNA-binding and unwinding to ATP hydrolysis (5,6,9,12). We reasoned that if the aromatic-rich loop in *E.coli* RecQ is functionally similar to that of PcrA, it would similarly link the enzyme's ATPase activity and its DNA-binding and unwinding functions. In support of this hypothesis, our data show that individual mutation of three different residues within this aromatic-rich loop lead to profound catalytic deficiencies, producing variants with uncoupled ATP hydrolysis and DNA unwinding activities.

Our results are consistent with a model in which the aromatic-rich loop in RecQ plays a similar role to the aromatic-rich loop in PcrA-related helicases. First, each of the mutated RecQ proteins has defects in DNA-dependent ATP hydrolysis and either requires higher concentrations of ssDNA to stimulate activity (W154L and R159L) or displays a greatly reduced need for DNA as a cofactor in ATPase activity (F158L) (Figure 2). Since each RecQ variant binds ssDNA with apparent WT affinity (Figure 3) and binds and hydrolyzes ATP with similar maximal efficiencies to that of WT RecQ (Table 1), the effect of the mutations appears to be a coupling deficiency in which DNA-binding inefficiently triggers ATP hydrolysis. Second, each of the three mutations produces a RecQ variant with greatly reduced DNA helicase activity (Figure 4), despite the fact that these proteins are competent to bind the partial-duplex substrate with WT affinity and can hydrolyze ATP. Thus, mutations in RecQ's aromatic-rich loop greatly impair the enzyme's ability to productively use the energy of ATP hydrolysis for DNA unwinding. With some exceptions described below, these effects are similar to those seen in aromatic-rich loop mutations within PcrA (5,6).

In spite of the structural similarities between the aromatic-rich loops of RecQ and PcrA-related enzymes and the functional similarities described in this report, there are some clear differences between the two loops that imply they have overlapping but non-identical functions. First, mutations of the aromatic-rich loop in RecQ do not affect binding affinity for ssDNA or 3′OH, whereas similar mutations in PcrA lead to DNA-binding defects (5,6). This difference implies that the aromatic-rich loop does not constitute the major DNA-binding determinant in RecQ, but instead other elements of the structure, such as the RecQ-Ct and HRDC domains (14,22–24), could form the major contact surfaces. Though it is possible that combinations of the single-site mutations could lead to a measurable difference in DNA-binding affinity, it appears that a simple DNA-binding defect cannot account for the differences in DNA-dependent ATPase and helicase activities of the variants. Second, the F158L variant has a significant DNA-independent ATPase activity, in stark contrast to the strong DNA dependence of WT RecQ ATPase activity (Figure 2A and B). To our knowledge, similar mutants have not been observed in PcrA-related or other SF-1 helicases. Interestingly, both the W154L and R159L mutations also appear to mildly stimulate DNA-independent ATPase activity over WT RecQ, although to a much lesser degree than that displayed by the F158L variant (Figure 2B). These results suggest that a DNA cofactor acts with RecQ to facilitate ATP hydrolysis, perhaps through a DNA-dependent conformational change in the protein that is mediated by the aromatic-rich loop. This structural alteration must be subtle, since we did not detect large-scale conformational changes induced by mutation or DNA-binding (Supplementary Figure 1 and data not shown). The ability of the F158L variant to hydrolyze ATP independently of a DNA cofactor could indicate that this variant mimics a DNA-bound state of RecQ. Together, these data imply that the RecQ aromatic-rich loop suppresses the enzyme's intrinsic ATPase activity, and that DNA-binding or mutation of the aromatic-rich loop releases this suppression. A third difference is that, unlike the aromatic-rich loop in PcrA, the aromatic-rich loop in RecQ does not directly contact nucleotide in the structure (14). This implies that the functions of the aromatic-rich loop in RecQ are likely to be indirect, and that subtle conformational changes within the aromatic-rich loop could allosterically activate the ATP hydrolysis active site. Alternatively, DNA-binding-induced conformational changes in the aromatic-rich loop could alter its position relative to ATP, allowing elements of the loop to directly participate in the ATP binding or hydrolysis, or could alter the position of motif II (adjacent to the aromatic-rich loop) to enhance its role in RecQ ATPase function. In addition, since the active oligomeric state of RecQ proteins remains unclear (25,26), it is also possible that the aromatic-rich loop acts *in trans* to activate ATP hydrolysis across a homotypic interface.

Based on the results presented here, we propose a model for the role of the aromatic-rich loop in RecQ's mechanism of DNA unwinding (Figure 5). Comparison of the crystal structures of apo- and ATPγS-bound RecQ shows only minor conformational differences (14), indicating that, before DNA contact, RecQ is competent to bind ATP. Hydrolysis of ATP in this state is very weak (Figure 2). When RecQ binds a partial-duplex substrate such as 3′OH DNA, the duplex portion of the DNA is thought to bind to the RecQ-Ct domain of the protein with the 3′ ssDNA tail binding across the face of the helicase domain as has been observed in other helicase structures (14). A model depicting this putative association is shown in Figure 5A. Our proposed mechanism predicts that ssDNA-binding to the RecQ helicase domain involves interaction between the DNA and the aromatic-rich loop and that, upon binding DNA, the loop conformation is subtly altered. As the conformation of the aromatic-rich loop is altered, the relative orientations of the two helicase lobes could also be altered, causing the enzyme to assume a conformation that is competent to hydrolyze the bound ATP. The specifics of this reorientation are unclear and could depend upon interactions between the aromatic-rich loop and the second major helicase domain ('Lobe 2' in Figure 5A). Consistent with this hypothesis, a hydrogen bond contact between a residue in the aromatic-rich loop and helicase motif VI of the second helicase domain is observed in the ATPγS-bound but not the apo-RecQ crystal structure (14), indicating that the aromatic-rich loop can conditionally link the two domains . Upon ATP hydrolysis and/or ADP release, the two helicase domain lobes could reorient and, in the process, translocate the enzyme

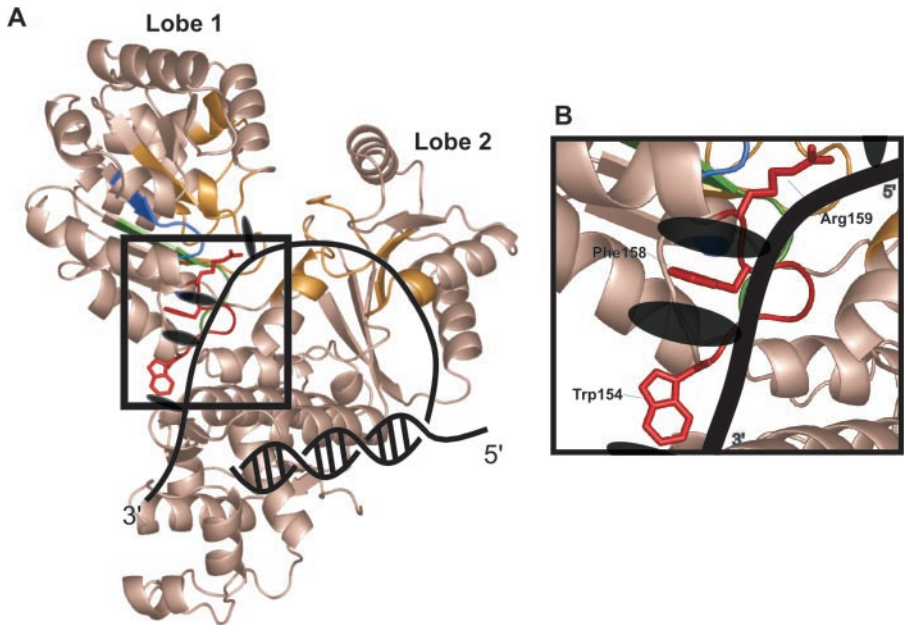

Figure 5. Proposed role of Trp154, Phe158 and Arg159 in RecQ catalytic activity. (**A**) *E.coli* RecQ catalytic core is shown with the residues from the RecQ aromatic-rich loop highlighted in red. This structure shows three lobes, the first two of which comprise the helicase domain (top left- and right-most lobes), while the third is the RecQ conserved domain (bottom lobe). The RecQ HRDC domain is not included in this structure. DNA is shown in black and individual DNA bases interacting with the aromatic-rich loop are represented schematically by black ovals. The image is colored as in Figure 1. (**B**) Close-up of model shown in (A). Residues of interest are labeled and the image is colored as in Figure 1.

along the ssDNA tail, unwinding the duplex DNA at a site distal to the aromatic-rich loop. DNA can interact once more with the aromatic-rich loop, thereby resetting the translocation cycle. This model is largely based on the inchworm model proposed for PcrA (12) in which residues from the aromatic-rich loop slide along the unwound ssDNA between each unwinding step and interact with the DNA during translocation.

In this report, we have presented evidence that *E.coli* RecQ uses an aromatic-rich loop within its helicase domain to couple ATP hydrolysis to DNA-binding/unwinding and have proposed a model wherein aromatic residues in the RecQ aromatic-rich loop stack with nucleotide bases of ssDNA. This idea is in contrast to other proposed SF-2 helicase mechanisms that rely primarily on protein interactions with the nucleic acid backbone (27,28) and instead resembles the proposed mechanisms of SF-1 helicases. Consistent with our model, two human RecQ proteins have also been recently proposed to act via SF-1-like mechanisms based on inhibition of their unwinding activities on DNA substrates with reduced backbone flexibility (29). RecQ proteins may therefore act in a manner that is distinct from other SF-2 helicases. Further studies examining the structural basis of RecQ DNA-binding and unwinding will be necessary to better define its precise mechanism of action.

SUPPLEMENTARY DATA

Supplementary Data are available at NAR Online.

ACKNOWLEDGEMENTS

We thank C.E. Berndsen and J.M. Denu for assistance with kinetic measurements and analysis and the members of the Keck lab for critical reading of the manuscript. This work was supported by a grant from the Shaw Foundation for Medical Research and National Institutes of Health grant GM068061 to J.L.K. Funding to pay the Open Access publication charges for this article was provided by National Institutes of Health grant GM068061.

Conflict of interest statement. None declared.

REFERENCES

1. Gorbalenya,A.E. and Koonin,E.V. (1993) Helicases: amino acid sequence comparisons and structure-function relationships. *Curr. Opin. Struct. Biol.*, **3**, 419–429.
2. Singleton,M.R. and Wigley,D.B. (2002) Modularity and specialization in superfamily 1 and 2 helicases. *J. Bacteriol.*, **184**, 1819–1826.
3. Caruthers,J.M. and McKay,D.B. (2002) Helicase structure and mechanism. *Curr. Opin. Struct. Biol.*, **12**, 123–133.
4. Subramanya,H.S., Bird,L.E., Brannigan,J.A. and Wigley,D.B. (1996) Crystal structure of a DExx box DNA helicase. *Nature*, **384**, 379–383.
5. Dillingham,M.S., Soultanas,P., Wiley,P., Webb,M.R. and Wigley,D.B. (2001) Defining the roles of individual residues in the single-stranded DNA binding site of PcrA helicase. *Proc. Natl Acad. Sci. USA*, **98**, 8381–8387.
6. Dillingham,M.S., Soultanas,P. and Wigley,D.B. (1999) Site-directed mutagenesis of motif III in PcrA helicase reveals a role in coupling ATP hydrolysis to strand separation. *Nucleic Acids Res.*, **27**, 3310–3317.
7. Soultanas,P., Dillingham,M.S., Velankar,S.S. and Wigley,D.B. (1999) DNA binding mediates conformational changes and metal ion coordination in the active site of PcrA helicase. *J. Mol. Biol.*, **290**, 137–148.
8. Soultanas,P., Dillingham,M.S., Wiley,P., Webb,M.R. and Wigley,D.B. (2000) Uncoupling DNA translocation and helicase activity in PcrA: direct evidence for an active mechanism. *EMBO. J.*, **19**, 3799–3810.
9. Korolev,S., Hsieh,J., Gauss,G.H., Lohman,T.M. and Waksman,G. (1997) Major domain swiveling revealed by the crystal structures of complexes of *E.coli* Rep helicase bound to single-stranded DNA and ADP. *Cell*, **90**, 635–647.

10. Brosh,R.M.,Jr and Matson,S.W. (1996) A partially functional DNA helicase II mutant defective in forming stable binary complexes with ATP and DNA. A role for helicase motif III. *J. Biol. Chem.*, **271**, 25360–25368.
11. Brosh,R.M.,Jr. and Matson,S.W. (1997) A point mutation in *Escherichia coli* DNA helicase II renders the enzyme nonfunctional in two DNA repair pathways. Evidence for initiation of unwinding from a nick *in vivo*. *J. Biol. Chem.*, **272**, 572–579.
12. Velankar,S.S., Soultanas,P., Dillingham,M.S., Subramanya,H.S. and Wigley,D.B. (1999) Crystal structures of complexes of PcrA DNA helicase with a DNA substrate indicate an inchworm mechanism. *Cell*, **97**, 75–84.
13. Singleton,M.R., Dillingham,M.S., Gaudier,M., Kowalczykowski,S.C. and Wigley,D.B. (2004) Crystal structure of RecBCD enzyme reveals a machine for processing DNA breaks. *Nature*, **432**, 187–193.
14. Bernstein,D.A., Zittel,M.C. and Keck,J.L. (2003) High-resolution structure of the *E.coli* RecQ helicase catalytic core. *EMBO J.*, **22**, 4910–4921.
15. Bernstein,D.A. and Keck,J.L. (2003) Domain mapping of *Escherichia coli* RecQ defines the roles of conserved N- and C-terminal regions in the RecQ family. *Nucleic Acids Res.*, **31**, 2778–2785.
16. Sambrook,J. and Russell,D.W. (2001) *Molecular Cloning: A Laboratory Manual, 3rd edn*. Cold Spring Harbor Laboratory Press, Cold Spring Harbor, NY.
17. Edelhoch,H. (1967) Spectroscopic determination of tryptophan and tyrosine in proteins. *Biochemistry*, **6**, 1948–1954.
18. Morrical,S.W., Lee,J. and Cox,M.M. (1986) Continuous association of *Escherichia coli* single-stranded DNA binding protein with stable complexes of recA protein and single-stranded DNA. *Biochemistry*, **25**, 1482–1494.
19. Umezu,K., Nakayama,K. and Nakayama,H. (1990) *Escherichia coli* RecQ protein is a DNA helicase [Erratum (1990) *Proc. Natl Acad. Sci. USA*, **87**, 9072.]. *Proc. Natl Acad. Sci. USA*, **87**, 5363–5367.
20. Harmon,F.G. and Kowalczykowski,S.C. (1998) RecQ helicase, in concert with RecA and SSB proteins, initiates and disrupts DNA recombination. *Genes Dev.*, **12**, 1134–1144.
21. Chao,K. and Lohman,T.M. (1990) DNA and nucleotide-induced conformational changes in the *Escherichia coli* Rep and helicase II (UvrD) proteins. *J. Biol. Chem.*, **265**, 1067–1076.
22. Bernstein,D.A. and Keck,J.L. (2005) Conferring substrate specificity to DNA helicases: role of the RecQ HRDC domain. *Structure (Camb)*, **13**, 1173–1182.
23. von Kobbe,C., Thoma,N.H., Czyzewski,B.K., Pavletich,N.P. and Bohr,V.A. (2003) Werner syndrome protein contains three structure-specific DNA binding domains. *J. Biol. Chem.*, **278**, 52997–53006.
24. Lee,J.W., Kusumoto,R., Doherty,K.M., Lin,G.X., Zeng,W., Cheng,W.H., von Kobbe,C., Brosh,R.M.Jr, Hu,J.S. and Bohr,V.A. (2005) Modulation of Werner syndrome protein function by a single mutation in the conserved RQC domain. *J. Biol. Chem*, **280**, 39627–39636.
25. Harmon,F.G. and Kowalczykowski,S.C. (2001) Biochemical characterization of the DNA helicase activity of the *Escherichia coli* RecQ helicase. *J. Biol. Chem.*, **276**, 232–243.
26. Xu,H.Q., Deprez,E., Zhang,A.H., Tauc,P., Ladjimi,M.M., Brochon,J.C., Auclair,C. and Xi,X.G. (2003) The *Escherichia coli* RecQ helicase functions as a monomer. *J. Biol. Chem.*, **278**, 34925–34933.
27. Singleton,M.R., Scaife,S. and Wigley,D.B. (2001) Structural analysis of DNA replication fork reversal by RecG. *Cell*, **107**, 79–89.
28. Kawaoka,J., Jankowsky,E. and Pyle,A.M. (2004) Backbone tracking by the SF2 helicase NPH-II. *Nature Struct. Mol. Biol.*, **11**, 526–530.
29. Garcia,P.L., Bradley,G., Hayes,C.J., Krintel,S., Soultanas,P. and Janscak,P. (2004) RPA alleviates the inhibitory effect of vinylphosphonate internucleotide linkages on DNA unwinding by BLM and WRN helicases. *Nucleic Acids Res.*, **32**, 3771–3778.
30. Holm,L. and Sander,C. (1996) Mapping the protein universe. *Science*, **273**, 595–603.
31. Caruthers,J.M., Johnson,E.R. and McKay,D.B. (2000) Crystal structure of yeast initiation factor 4A, a DEAD-box RNA helicase. *Proc. Natl Acad. Sci. USA*, **97**, 13080–13085.
32. Carmel,A.B. and Matthews,B.W. (2004) Crystal structure of the BstDEAD N-terminal domain: a novel DEAD protein from *Bacillus stearothermophilus*. *RNA*, **10**, 66–74.